Electronic Supplementary Material (ESI) for Lab on a Chip.

Supplementary information

Efficient full-length IgG secretion and sorting from single yeast clones in droplet PicoReactors

Esteban Lebrun,[ab] Vasily Shenshin,[a] Cécile Plaire,[a] Vincent Vigneres,[c] Théo Pizette,[a] Bruno Dumas,[a] Jean-Marc Nicaud[b‡] and Guillaume Mottet*[a‡]

[a.] *Large Molecules Research, Sanofi, 94400 Vitry-Sur-Seine, France.*

[b.] *Université Paris-Saclay, INRAE, AgroParisTech, Micalis Institute, 78350 Jouy-en-Josas, France.*

[c.] *Arcale, 31100 Toulouse, France.*

* Corresponding author.

‡ These authors jointly supervised the work.

Supplementary Table 1. Main *E. coli* strains used in this work.

Strain	Genotype, characteristics	Reference / Origin
<u>*E. coli* strains</u>		
DH5α	F- Φ80*lac*ZΔM15 Δ(*lac*ZYA-*arg*F) U169 *rec*A1 *end*A1 *hsd*R17(rk-, mk+) *pho*A *sup*E44 *thi*-1 *gyr*A96 *rel*A1 λ-	Invitrogen
<u>Plasmids stored in *E. coli*</u>		
pCR-Blunt II-TOPO	ColE1-ori KanR, destination vector	Invitrogen
GGE114	pSB1A3-ZetaUP-*URA3*ex-RFP-ZetaDOWN, destination vector	Celińska *et al.*, 2017[1]
GGE 0020	pCR4Blunt-TOPO T1-3_Lip2	Celińska *et al.*, 2017[1]
GGE0146	pCR4Blunt-TOPO P1_TEF-4UASxpr2	Larroude *et al.*, 2019[2]
GGE0270	pCR4Blunt-TOPO G1_YFP	Larroude *et al.*, 2019[2]
JME4393	GGA_CrisprCas9-yl_sgRNA platform-RFP_*LYS5*_p8UASxpr2TEF	Larroude *et al.*, 2020[3]
JME4889	TOPO-BDP-pEYK450-5AB-Fw	Vidal *et al.*, 2023[4]
GGE0429	GGE114 tXpr2_CL_AmilCP_CH_tLip2	This work
GGE0431	GGE429 OKT3-VL_RFP_OKT3-VH	This work
GGE0440	JME4393 sgRNA-Fila	This work
JME5595	GGE448 pTEF_YFP_tLip2	This work
GGE0468	pCR-Blunt II-TOPO SP4_pEYK(450)-5AB_SP1	This work
GGE0472	pCR-Blunt II-TOPO SP3_pEYK(450)-5AB_SP6	This work
GGE0448	pSB1A3_ZetaUP-*LYS5*ex-RFP-ZetaDOWN, destination vector	This work
JME5358	GGE448 Zeta-Lys5Ex-p4UASxpr2-coreTEF-PDI-tLip2-Zeta	This work
JME5359	GGE448 Zeta-Lys5Ex-p4UASxpr2-coreTEF-ERO1-tLip2-Zeta	This work
JME5360	GGE448 Zeta-Lys5Ex-p4UASxpr2-coreTEF-BiP-tLip2-Zeta	This work
JME5361	GGE448 Zeta-Lys5Ex-p4UASxpr2-coreTEF-HAC1-tLip2-Zeta	This work
JME5362	GGE448 Zeta-Lys5Ex-p4UASxpr2-coreTEF-SLS1-tLip2-Zeta	This work
JME5559	GGE114 OKT3_SP4-SP1 L/Hgly+cys	This work
JME5560	GGE114 OKT3_SP4-SP1 Lgly/Hcys	This work
JME5561	GGE114 OKT3_SP4-SP1 L/Hcys	This work
JME5562	GGE114 OKT3_SP4-SP1 L/Hgly	This work
JME5563	GGE114 OKT3_SP4-SP1 L/H	This work
JME5546	GGE429 FUN1-VL_SP4-SP1_FUN1-VH	This work
JME5710	GGE429 OKT3-VL_SP4-SP1_OKT3-VH	This work
JME5711	GGE429 TNP-VL_SP3-SP6_TNP-VH	This work
JME5712	GGE429 CD3blina-VL_SP4-SP1_CD3blina-VH	This work
JME5713	GGE429 CD3tepli-VL_SP4-SP1_CD3tepli-VH	This work
JME5714	GGE429 UCHT1-VL_SP4-SP1_UCHT1-VH	This work

Supplementary Table 2. Main *Y. lipolytica* strains used in this work.

Strain	Genotype, characteristics	Reference / Origin
Y. lipolytica strains		
JMY7126	*MATA*, *ura3-302*, *leu2-270-LEU2*-Zeta, *xpr2-322*, *lip2*Δ, *lip7*Δ, *lip8*Δ, *lys5*Δ, *eyk1*Δ	Park *et al.*, 2019[5]
JMY9315	JMY7126 *URA3* TNP_SP3-SP6	This work
JMY9316	JMY7126 *URA3* CD3blina_SP4-SP1	This work
JMY9317	JMY7126 *URA3* CD3tepli_SP4-SP1	This work
JMY9318	JMY7126 *URA3* UCHT1_SP4-SP1	This work
JMY9320	JMY7126 *URA3* OKT3_SP4-SP1	This work
JMY8662	JMY7126 *URA3 LYS5*	This work
JMY8660	JMY7126 *URA3 LYS5* OKT3_SP4-SP1	This work
JMY8655	JMY7126 *URA3 LYS5* OKT3_SP4-SP1 ylPDI	This work
JMY8658	JMY7126 *URA3 LYS5* OKT3_SP4-SP1 huPDI	This work
JMY8701	JMY7126 *URA3 LYS5* OKT3_SP4-SP1 ERO1	This work
JMY8702	JMY7126 *URA3 LYS5* OKT3_SP4-SP1 BiP	This work
JMY8703	JMY7126 *URA3 LYS5* OKT3_SP4-SP1 HAC1	This work
JMY8704	JMY7126 *URA3 LYS5* OKT3_SP4-SP1 SLS1	This work
ELY12-2	JMY7126 *URA3* OKT3_SP4-SP1_L/Hgly+cys	This work
ELY12-3	JMY7126 *URA3* OKT3_SP4-SP1_Lgly/Hcys	This work
ELY12-4	JMY7126 *URA3* OKT3_SP4-SP1_L/Hcys	This work
ELY12-5	JMY7126 *URA3* OKT3_SP4-SP1_L/Hgly	This work
ELY12-6	JMY7126 *URA3* OKT3_SP4-SP1_L/H	This work
JMY8647	JMY7126 *mhy1*Δ	This work
JMY8651	JMY8647 *URA3*	This work
JMY8652	JMY8647 *URA3* OKT3_SP4-SP1	This work
JMY9321	JMY8647 *URA3* FUN1_SP4-SP1	This work
JMY9322	JMY8647 *URA3* TNP_SP3-SP6	This work
JMY9393	JMY8647 *URA3* FUN1_SP4-SP1 YFP	This work
JMY9394	JMY8647 *URA3* TNP_SP3-SP6 YFP	This work
JMY9395	JMY8647 *URA3* YFP	This work

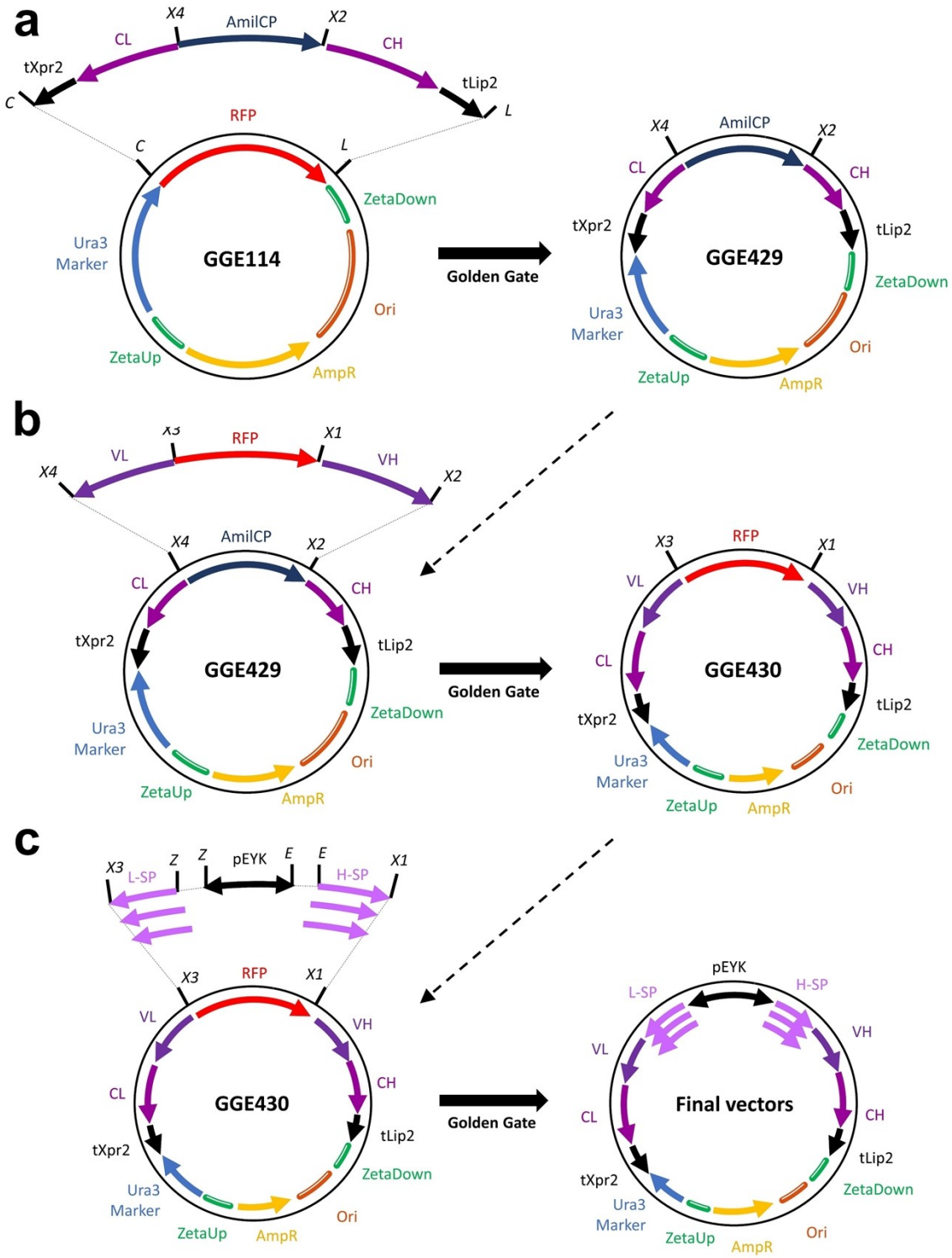

Supplementary Figure 1. Cloning workflow of antibody expression cassettes. (**a**) The constant sequences of an IgG1-kappa antibody were cloned with genetic terminators in opposite directions into GGE114 to create the plasmid GGE429. The Golden Gate assembly used *C* and *L BsaI* restriction sites. The *RFP* gene removal allowed transformants selection. (**b**) The variable sequences of the antibody OKT3 were cloned into GGE429 to create the plasmid GGE430. The Golden Gate assembly used *X4* and *X2 BsaI* restriction sites. The *AmilCP* gene removal allowed transformants selection. (**c**) The promoter pEYK and two signal peptides were cloned between the light chain and the heavy chain of OKT3 to generate a library of IgG expression cassettes with unique SPs combinations. The Golden Gate assembly used *X3*, *Z*, *E*, and *X1 BsaI* restriction sites. The *RFP* gene removal allowed transformants selection.

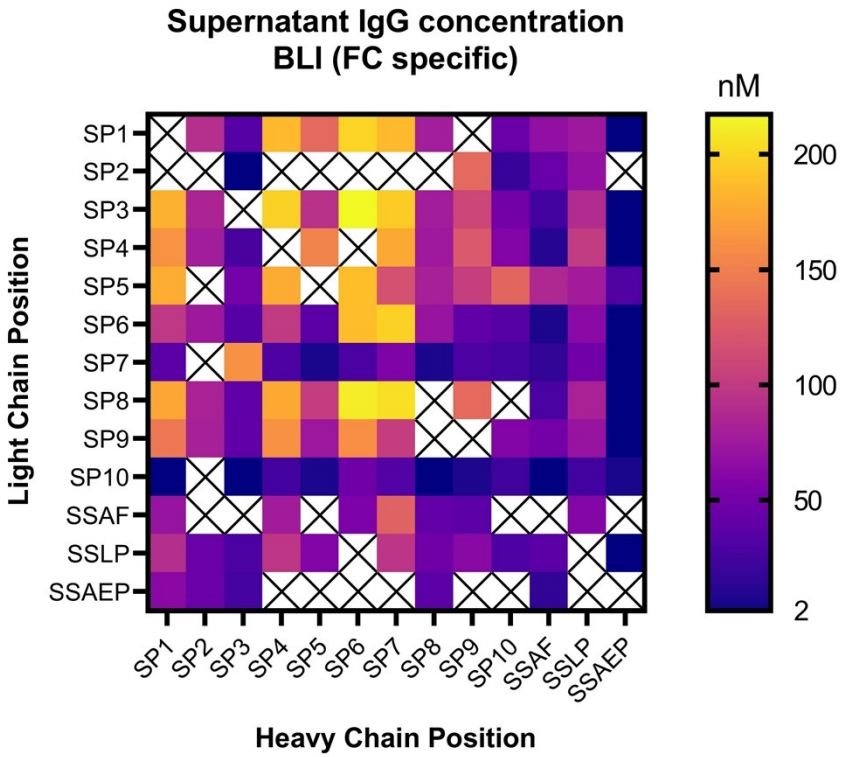

Supplementary Figure 2. Supernatant IgG concentration (BLI). Supernatant antibody fragments concentrations reached with 132 IgG expression cassettes after 48 hours of yeast cultivation. Supernatants were filtered, and antibody fragments concentrations were measured by BLI. Each box corresponds to a strain expressing an antibody production cassette with a unique SPs combination. The values are the mean of measured concentrations from up to 4 biological replicates. Crosses represent production cassettes that could not be constructed.

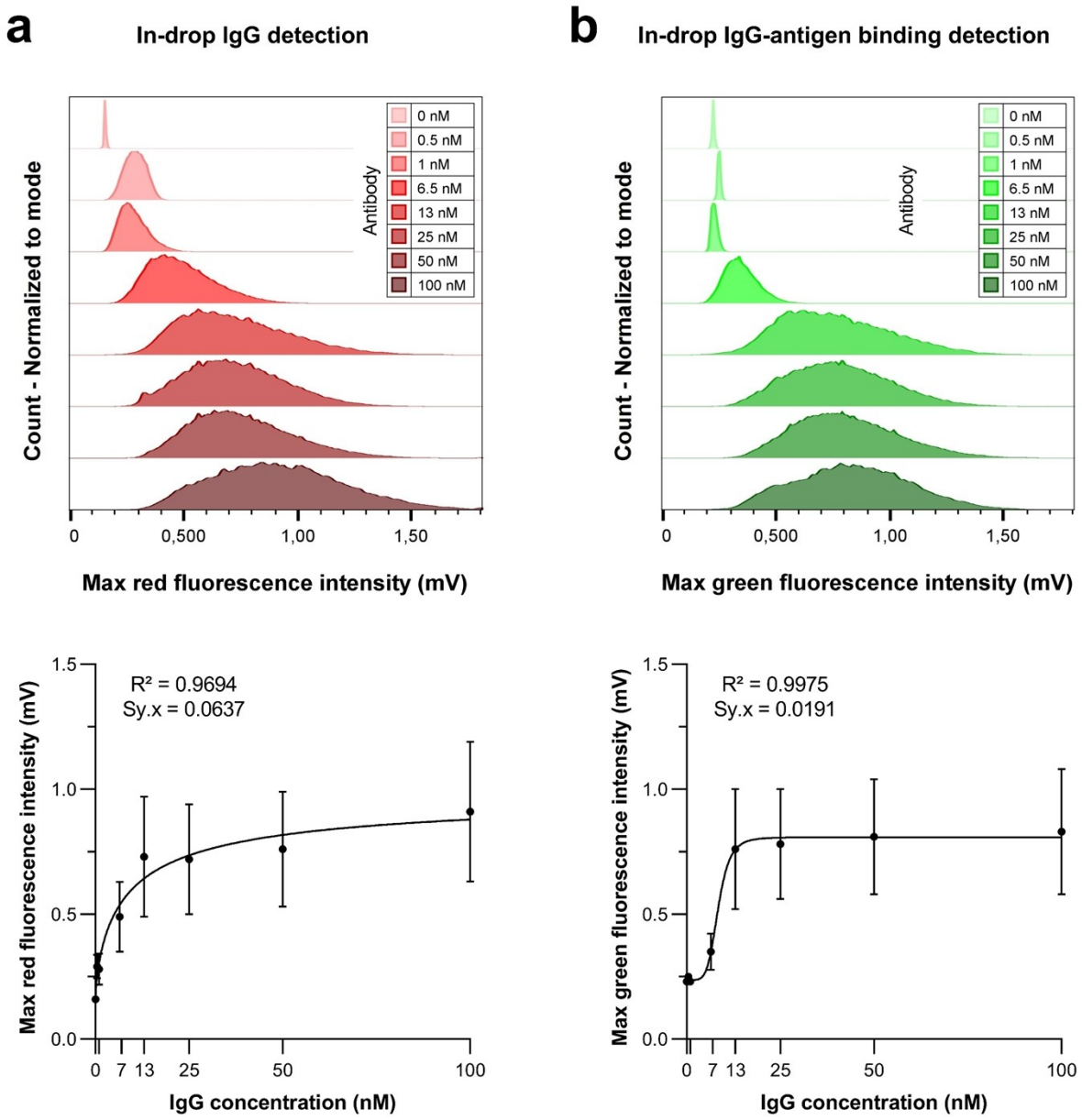

Supplementary Figure 3. IgG detection limits of microfluidic reading. Various concentrations of purified IgGs were separately encapsulated with bioassay material. Maximum in-drop red fluorescence (i.e., IgG detection) (**a**) and green fluorescence (i.e., IgG-antigen binding detection) (**b**) were read by laser scanning in a microfluidic chip. Upper panels show, for each condition, the count of drops harboring various levels of fluorescence. Lower panels show the mean ± SD maximum fluorescence per drop as a function of in-drop IgGs concentration. Non-linear regression is shown.

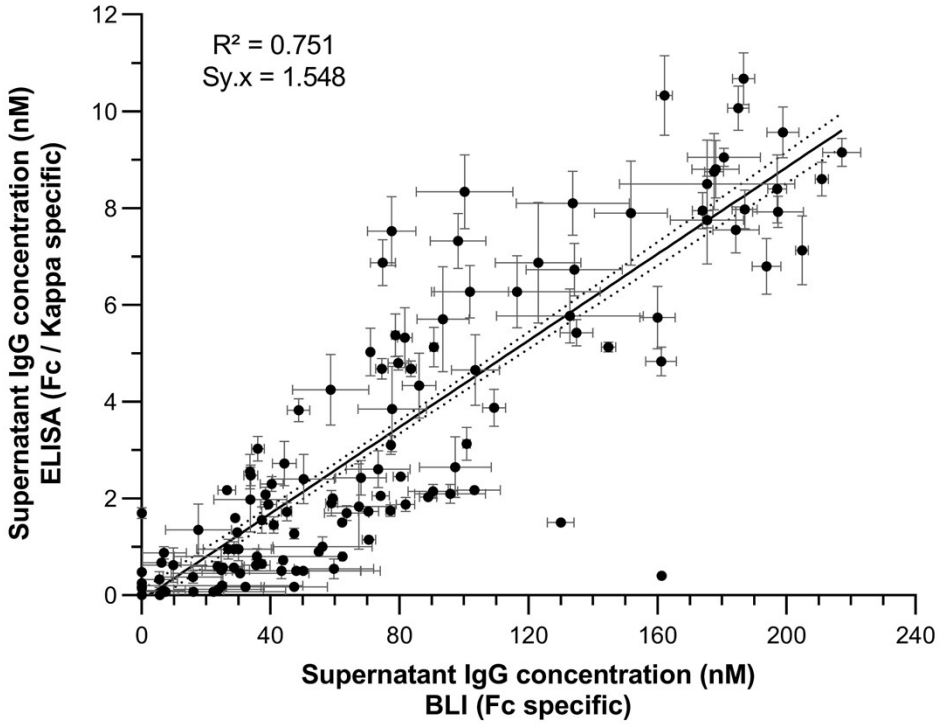

Supplementary Figure 4. Correlation between BLI and ELISA dosage of supernatant antibodies. Up to 4 clones of *Y. lipolytica* having each SPs combination were grown for 48 hours in YPD medium with inducer. The supernatants were filtered, and their antibody concentrations were measured by BLI and ELISA. Each dot represents the mean ± SEM concentration reached with one SPs combination. Simple linear regression is shown with 95% confidence bands.

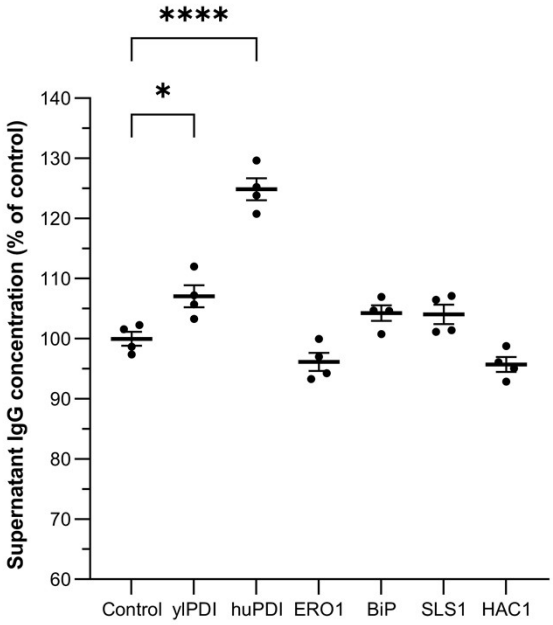

Supplementary Figure 5. Impact of helper genes overexpression on IgG secretion. Four clones of *Y. lipolytica* expressing the SP4-SP1 IgG expression cassette and overexpressing various proteins (chaperones and transcription factor) were grown for 48 hours in YPD medium with inducer. The supernatants were filtered, and their antibody concentrations were measured by ELISA. The mean ± SEM is shown. Ordinary one-way ANOVA, P value < 0.0332 (*) or < 0.0001 (****).

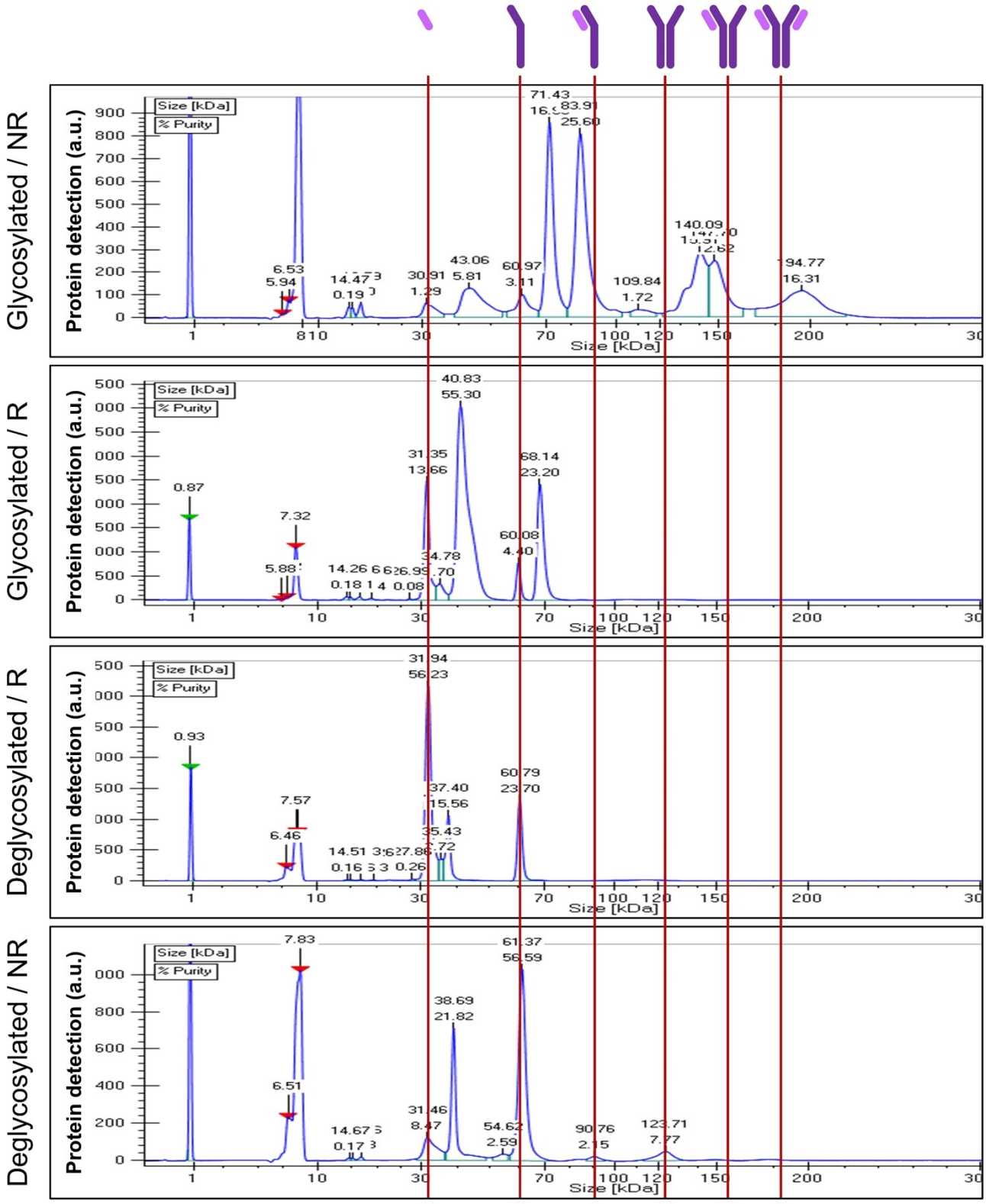

Supplementary Figure 6. Composition of the antibody fragments mixture in a yeast culture supernatant. The SPs combination SP4-SP1 was used to produce OKT3, and the supernatant was filtered. Antibody fragments were purified on Protein A resin, deglycosylated or not with PNGase, and read by capillary electrophoresis. The 37-38 kDa peak corresponds to PNGase. The 15 kDa peak is an experimental artifact. Red lines indicate the expected size of fully-assembled and partially-assembled IgGs. R: reducing conditions; NR: non-reducing conditions.

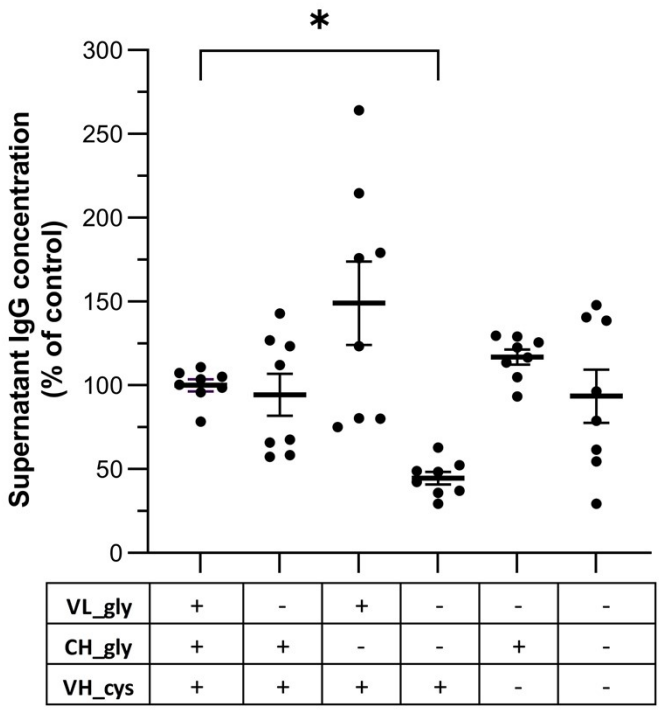

Supplementary Figure 7. Impact of OKT3's glycosylation sites and free cysteine removal on IgG secretion. Eight clones of *Y. lipolytica* expressing each variant of the SP4-SP1 IgG expression cassette were grown for 48 hours in YPD medium with inducer. VL_gly: glycosylation site in the VL; CH_gly: glycosylation site in the CH; VH_cys: free cysteine in the VH. The supernatants were filtered, and their antibody concentrations were measured by ELISA. The mean ± SEM is shown. Ordinary one-way ANOVA, P value < 0.0332 (*).

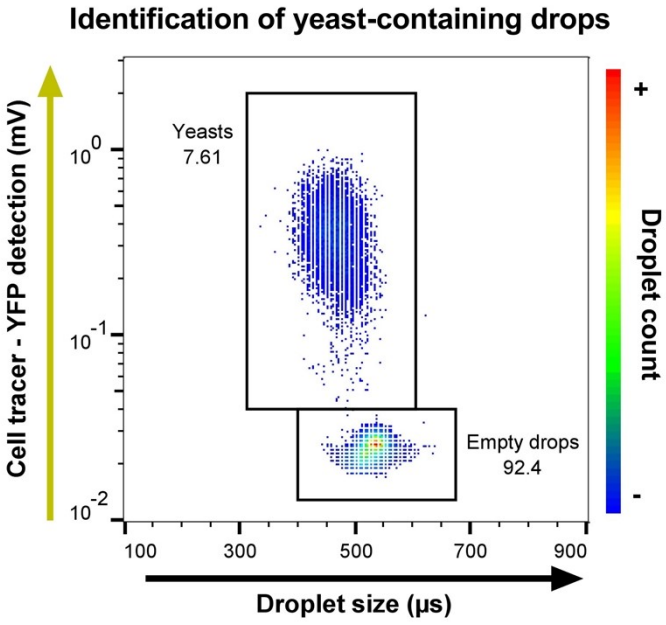

Supplementary Figure 8. Effect of yeast growth on droplet size. Heterologous fluorescence production was used to identify yeast-containing drops, and their average size was compared to that of empty drops. Density plot, each dot represents the signal from one read drop; the color represents the abundance of drops sharing the same characteristics.

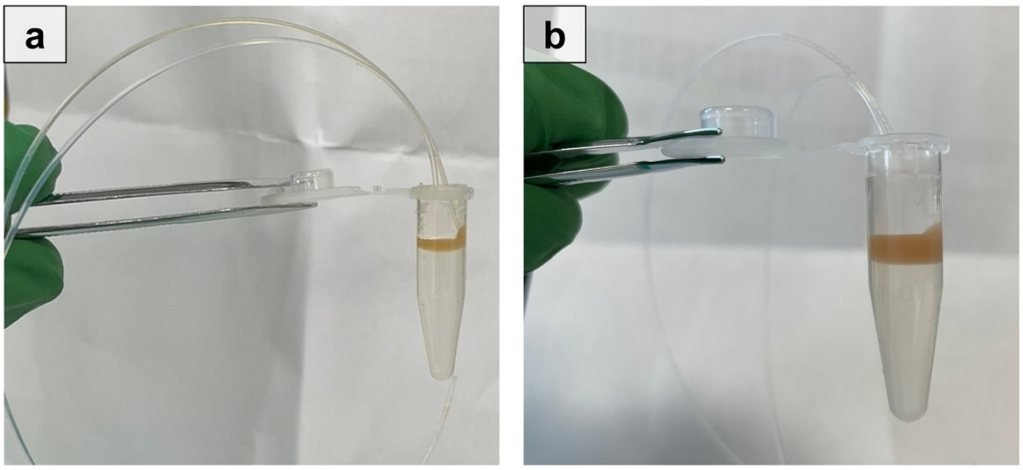

Supplementary Figure 9. Collecting tubes for emulsion incubation. (**a**) 0.5 mL tube for collecting small emulsions. If the volume of emulsion exceeds the volume of oil, the yeast's growth is affected by a lack of oxygen. (**b**) 1.5 mL tube for collecting large emulsions (up to 400 µL).

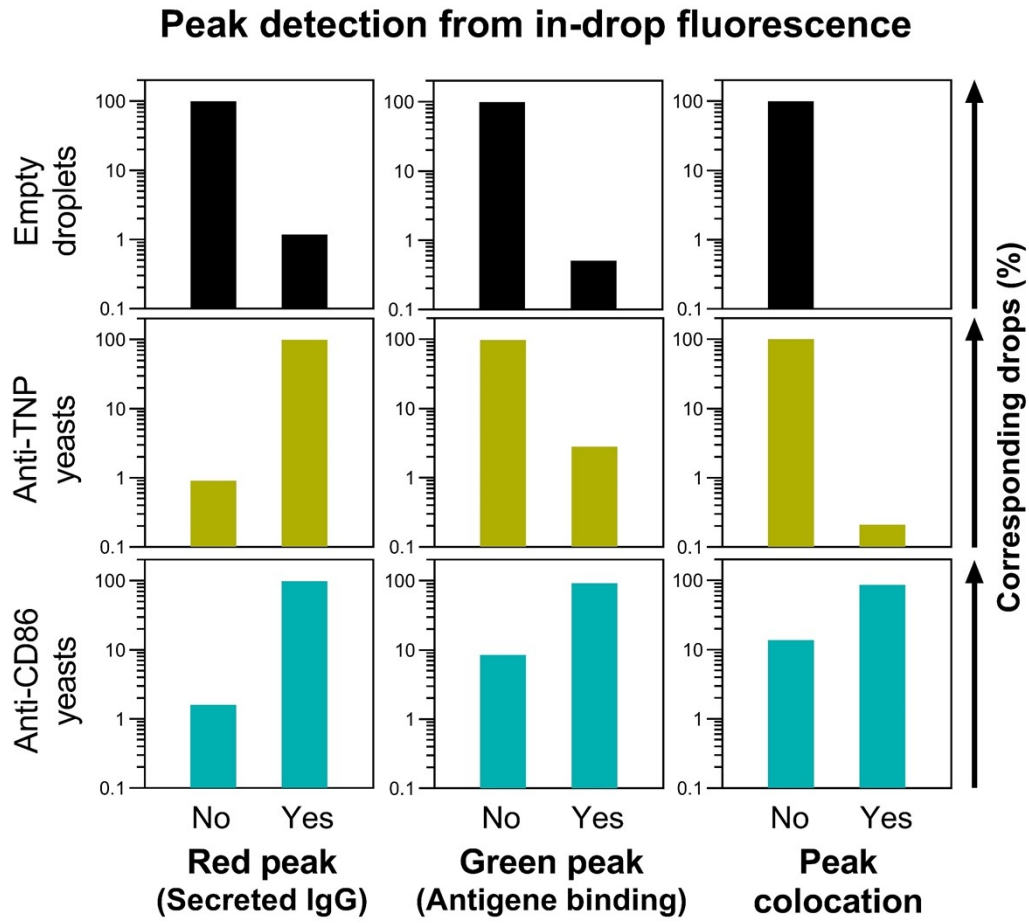

Supplementary Figure 10. Proportion of drops containing red or green fluorescence peaks among various populations. Upper panel: drops containing no yeasts; middle panel: drops containing yeasts that produce non-binder IgGs; lower panel: drops containing yeasts that produce binder IgGs.

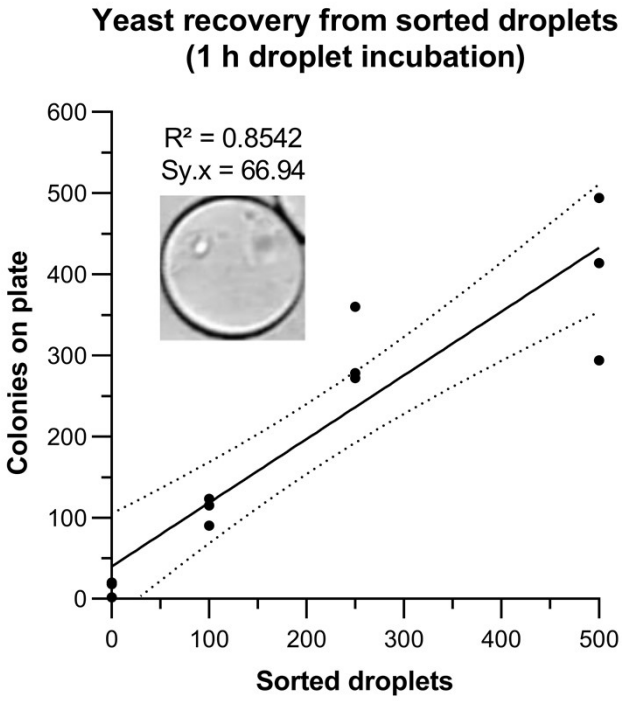

Supplementary Figure 11. Recovery tests of encapsulated yeasts after drop sorting. Drops containing one YFP-producing yeast were incubated for 1 hour, and various amounts of drops were sorted and spread on YPD-agarose plates. Recovered colonies were counted. Simple linear regression is shown with 95% confidence bands.

References

1 E. Celińska, R. Ledesma-Amaro, M. Larroude, T. Rossignol, C. Pauthenier and J.-M. Nicaud, Microb. Biotechnol., 2017, 10, 450–455.

2 M. Larroude, Y. Park, P. Soudier, M. Kubiak, J. Nicaud and T. Rossignol, Microb. Biotechnol., 2019, 12, 1249–1259.

3 M. Larroude, H. Trabelsi, J.-M. Nicaud and T. Rossignol, Biotechnol Lett, 2020, 42, 773–785.

4 L. Vidal, E. Lebrun, Y.-K. Park, G. Mottet and J.-M. Nicaud, Microb Cell Fact, 2023, 22, 7.

5 Y.-K. Park, M. Vandermies, P. Soudier, S. Telek, S. Thomas, J.-M. Nicaud and P. Fickers, Microb Cell Fact, 2019, 18, 167.